International Journal of Mass Spectrometry and Ion Processes, 87 (1989) 209–224
Elsevier Science Publishers B.V., Amsterdam – Printed in The Netherlands

DETERMINATION OF ABSOLUTE PARTIAL AND TOTAL ELECTRON IMPACT IONIZATION CROSS-SECTIONS FOR CF_2Cl_2 FROM THRESHOLD UP TO 180 eV: AN IMPROVED EXPERIMENTAL METHOD

K. LEITER *, P. SCHEIER, G. WALDER and T.D. MÄRK

Institut für Ionenphysik, Leopold Franzens Universität, A 6020 Innsbruck (Austria)

(First received 5 May 1988; in final form 6 June 1988)

ABSTRACT

Electron impact ionization of CF_2Cl_2 has been studied as a function of electron energy from threshold up to 180 eV using a double focussing sector field mass spectrometer (reversed geometry) with an improved ion transmission characteristic. With this set-up complete and/or controlled collection of mass selected parent and fragment ions can be achieved, thus permitting the accurate measurement of quantitative electron impact ionization cross-sections. Absolute partial ionization cross-section functions for the production of $CF_2Cl_2^+$, $CFCl_2^+$, CF_2Cl^+, CCl_2^+, Cl_2^+, $CFCl^+$, FCl^+, CF_2^+, CCl^+, Cl^+, CF^+, F^+, C^+, $CFCl_2^{2+}$, CF_2Cl^{2+}, $CFCl^{2+}$, CCl_2^{2+}, CCl^{2+} and Cl^{2+} have been determined. In addition, the total ionization cross-section function of CF_2Cl_2 is obtained and compared with previous experimental and theoretical results.

INTRODUCTION

Accurate absolute electron impact ionization cross-sections of atoms and molecules are required in many scientific areas, such as mass spectrometry, gas discharges, modelling of semiconductor processing, astrophysics and fusion technology [1]. In the last few years there has been a growing interest in the ionization properties of fluoro- and chloroalkanes (see also a recent review on cross-section measurements of radicals [2] and experimental determinations of fluorinated compounds [3]), in particular because of their applied relevance in the frame of plasma etching [4,5]. Partial and total electron impact ionization cross-section functions of CF_4 [6] and CCl_4 [7] have been recently measured in our laboratory.

* Present address: Fa. Ionentechnik, A 6176 Völs, Austria.

0168-1176/89/$03.50

The present study is devoted to CF_2Cl_2 using an improved ion beam deflection technique allowing quantitative measurement of not only parent ions but also ions with excess kinetic energy, e.g., fragment ions. Absolute partial ionization cross-section functions for the production of $CF_2Cl_2^+$, $CFCl_2^+$, CF_2Cl^+, CCl_2^+, Cl_2^+, $CFCl^+$, FCl^+, CF_2^+, CCl^+, Cl^+, CF^+, F^+, C^+, $CFCl_2^{2+}$, CF_2Cl^{2+}, $CFCl^{2+}$, CCl_2^{2+}, CCl^{2+} and Cl^{2+} have been determined. In addition, the total ionization cross-section function of CF_2Cl_2 is obtained and compared with previous experimental and theoretical results.

EXPERIMENTAL

Apparatus

The experimental set-up used consists of a conventional three-electrode type electron impact ion source, and a high-resolution double focussing (reversed geometry) sector field mass spectrometer. The properties of the ion source and mass spectrometer have been studied in detail previously and essential improvements in the performance could be achieved [8]. With the help of these improved operating conditions it was possible to measure with high accuracy absolute partial ionization cross-sections for atomic and molecular parent ions [8–10]. In recent studies [6,7] this method was extended to allow the measurement of partial ionization cross-section for fragment ions with excess kinetic energy. In the present study the method is further improved and the technique simplified (automatic y-deflection scan, see below).

Figure 1a gives a schematic view of the electron impact ion source and the ion extraction and focussing system used. The gas under study flows from a reservoir (in the gas handling system) through a 10 μm diameter nozzle N into the high vacuum region (background pressure ca. 10^{-7} torr). Approximately 20 mm downstream a fraction of the emerging molecular beam enters the collision chamber C through a 5-mm diameter aperture A and is crossed at right angles by an electron beam of variable energy (up to 180 eV). A 500 l s^{-1} turbomolecular pump evacuates the ion source chamber. The electron beam (with stabilized currents between 1 and 30 μA) is aligned by a weak magnetic field ($\approx$ 400 G). The energy spread of the electron beam is approximately 0.5 eV (FWHM) [8].

Ions formed by electron impact are extracted from the collision chamber through a slit in electrode L_1 (1.5-mm width in y direction (see Fig. 1a), 8-mm height in z direction) with the help of an electric field penetrating into the collision chamber from L_2. Electrode L_1, pusher P and the collision chamber C are kept at the same potential, typically +3kV (ion accelerating

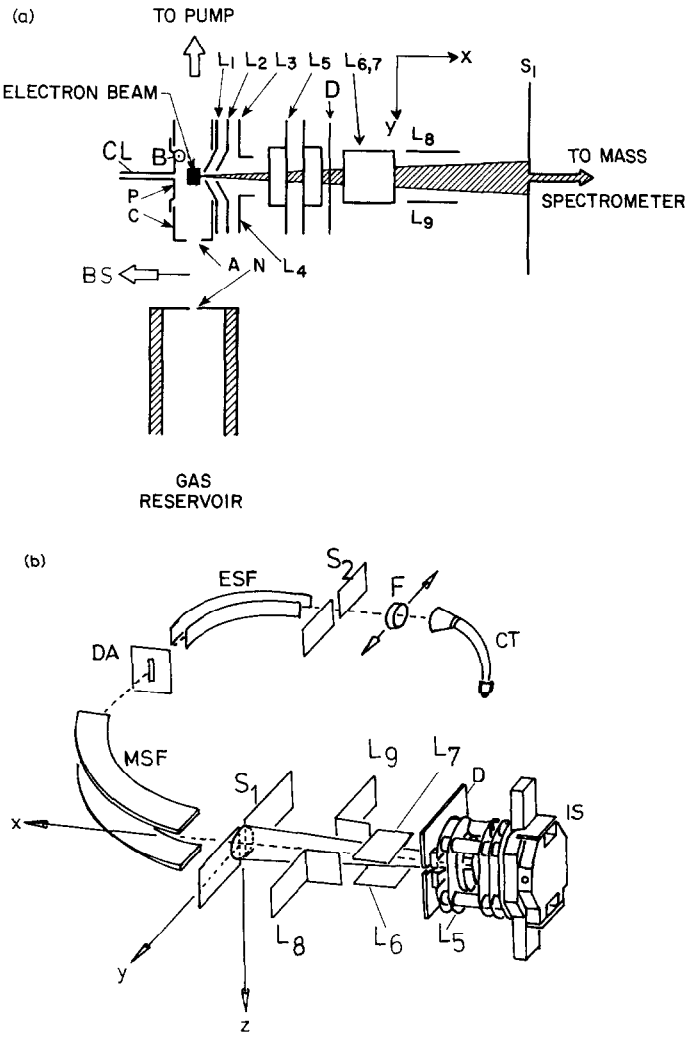

Fig. 1. Schematic view of (a) the electron impact ion source and (b) the double focussing mass spectrometer system used in the present study. P, pusher; C, collision chamber; CL, capillary leak gas inlet; A, aperture; N, nozzle for molecular beam gas inlet; BS, beam stop; B, magnetic field; L_1, collision chamber exit slit electrodes; L_2, penetrating field electrodes; L_3 and L_4, focussing electrodes; L_5, ground slit; D, defining aperture; L_6, L_7, L_8 and L_9, ion beam deflection electrodes; S_1, mass spectrometer entrance slit; z direction, perpendicular to the $x-y$ plane (right-hand axes); DA, defining aperture; S_2, mass spectrometer exit slit; F, Faraday cage; CT, channeltron; MSF, magnetic sector field; ESF, electric sector field.

voltage). L_3 and L_4 are used for beam centering and focussing, L_5 (earth slit) is the end of the accelerating region, and D is a defining aperture. Deflection plates L_6, L_7 and L_8, L_9 serve to sweep the extracted ion beam either parallel (z deflection) or perpendicular (y deflection) across the mass

spectrometer entrance slit S_1, respectively. The fraction of ions passing S_1 is analyzed in a 90° magnetic sector field followed by a 90° electric sector field (see Fig. 1b). In addition to a Faraday cup, which is used to measure absolute ion currents (in order to determine all absolute cross-sections and ratios; see below) a CuBe-conversion dynode followed by a channeltron is used as either analog or counting detector.

Measuring technique

In order to determine absolute partial ionization cross-sections it is necessary to uniquely correlate the mass analyzed ion signal at the ion collecting system to the number of ions produced in the ion source at a known target gas density and for a known electron beam current. This is a difficult task due to mass-to-charge dependent discrimination: (i) in the extraction of the ions from the ion source; and (ii) in the transmission of the mass spectrometer, i.e., through the entrance slit S_1. In order to avoid discrimination at the entrance slit S_1 it has been shown [8] that for ions without kinetic energy (parent ions) it is sufficient to sweep the extracted ion current with the help of $L_{8,9}$ perpendicular to S_1 and to integrate over the recorded y-ion beam profile. Figure 2 shows y-ion beam profiles for Ar^+, Ar^{2+}, and singly and doubly charged ions produced in CF_2Cl_2. It can clearly be seen that different ions have different beam shapes and positions in the y direction leading to discrimination without integration [8].

Because of negligible differences in z-ion beam profiles for parent ions no integration parallel to S_1 was necessary for the accurate measurements of these ions [8]. For fragment ions, however, discrimination in the z direction has also to be accounted for, because of large differences in the z-ion-beam profiles for the different fragment ion species. Figure 3 shows z-ion-beam profiles for some singly and doubly charged ions in CF_2Cl_2 and Ar. Without integration in the z direction large discrimination effects will occur in the detection efficiency of ions with different mass-to-charge ratio and different excess kinetic energy.

Recently, Stephan et al. [6] have shown for CF_4 that the overall ion beam shapes are essentially a product of the profiles in either direction. Thus, in order to account for the overall discrimination Stephan et al. [6] have demonstrated that it is sufficient to determine separately the profile in the z direction at one particular y value (e.g., $U_y = 0$ V) and the profile in the y direction at one particular z value (e.g., $U_z = 0$ V) and then integrate with the help of these two data sets over the whole beam shape. In the present study this integration method is improved by operating a 1 kHz sweep generator on the y-deflection plates during the z scan. It is then sufficient to integrate over this y-integrated z-ion-beam profile in order to obtain a

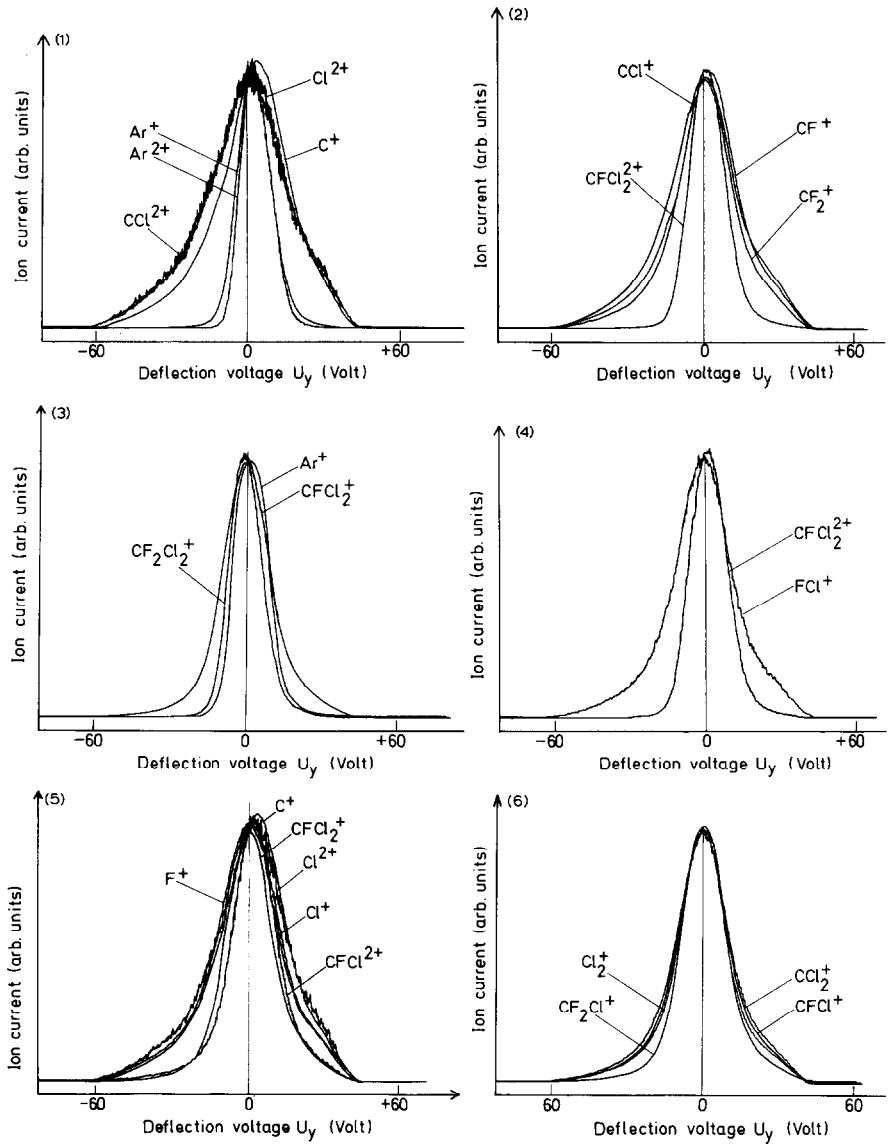

Fig. 2. Ion-beam profiles (deflection curves in y direction) of Ar^+, Ar^{2+}, and singly and doubly charged ions from CF_2Cl_2 obtained by sweeping the fanned out ion beam perpendicularly across the mass spectrometer entrance slit S_1 with the help of the deflection plates, L_8 and L_9 (see Fig. 1a) under strong focussing conditions of L_3 and L_4 [8]. It can be seen that the width of the fragment ion beam profiles in this y direction is increasing with decreasing ion mass, since the kinetic excess energy of dissociative ions with smaller mass is larger. Moreover, doubly charged fragment ions have a smaller ion beam profile than singly charged fragment ions (see ref. 8).

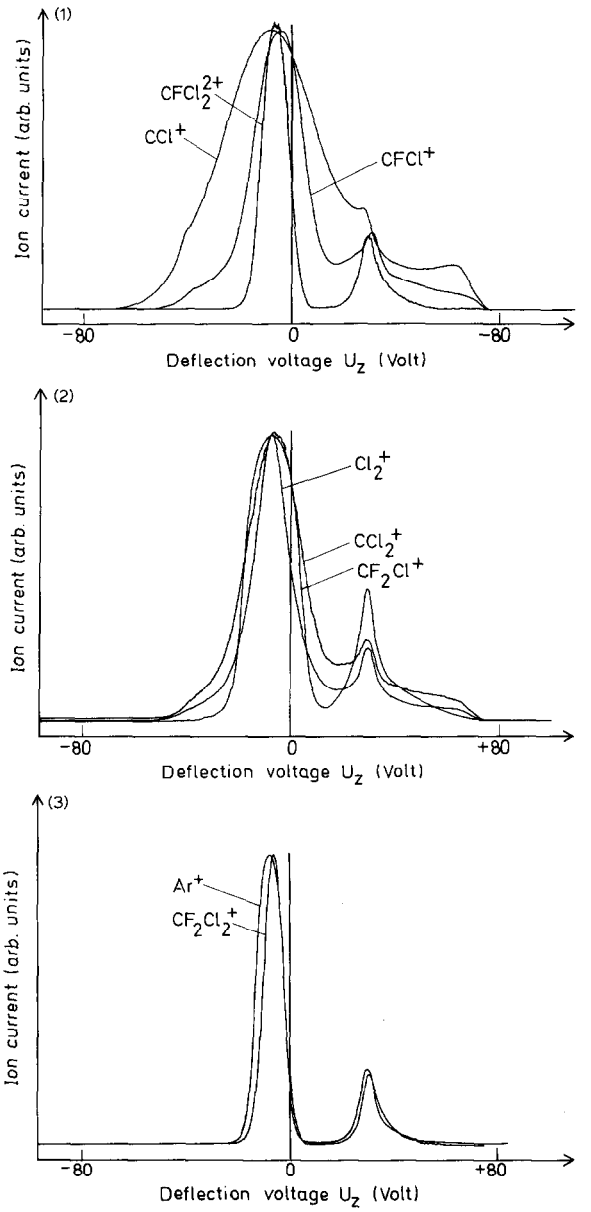

Fig. 3. Ion-beam profiles (deflection curves in z direction) of Ar^+ and singly and doubly charged ions from CF_2Cl_2 obtained by sweeping the fanned out ion beam across the mass spectrometer entrance slit S_1 with the help of the deflection plates $L_{6,7}$ under strong focussing conditions of L_3 and L_4 [8]. It can be seen that the width of the fragment ion beam profiles is increasing with decreasing ion mass, since the kinetic excess energy of dissociative ions with smaller mass is larger. Moreover, doubly charged fragment ions have a smaller ion beam profile than singly charged fragment ions. (See also difference between Ar^+ and Ar^{2+} profile in ref. 8.)

representative measure of the total ion current of the ion under study. The second (smaller) peak in the z profiles (see Fig. 3) is in the present study * not included in this integration process, because these ions originate from surface reaction in the ion source according to previous results [8].

This integration method is very well suited, and is also used here, for the determination of the total ion current and (using the calibration procedure described below) the absolute ionization cross-section at one electron energy. For the determination of the electron energy dependence of the cross-section this method is rather time consuming. Stephan et al. [8] and Leiter et al. [7], however, have shown that the z-ion beam profile of a specific ion does not change with electron energy. Conversely the y-ion beam profile changes with electron energy without special precautions [8]. Thus, relative ionization cross-section functions can be measured using the 1 kHz sweep generator on the y-deflection plates at any U_z position without taking a z scan (we have tested this procedure by measuring for several fragment ions complete sets of z scans, and by integrating at every electron energy). This method constitutes an important advantage over the previous techniques [6–8].

Moreover, it is not only necessary to avoid any discrimination at S_1, but it is also necessary to extract all ions of a specific species produced in the ion source in order to obtain reliable ion current ratios and/or cross-section ratios. Stephan et al. [8] have demonstrated that this is possible for parent ions, if the field penetration from lens L_2 into the collision chamber is strong enough and integration over the y-ion beam profiles is performed. In a recent investigation we have studied the extraction conditions for fragment ions and have shown [6,7] that mass analyzed y-integrated ion signals not only saturate for parent ions, but also for fragment ions if the potential difference between the collision chamber and lens L_2, U_{C-L_2}, is large enough. Only ions with very large excess kinetic energy do not saturate at the maximum possible voltage of 340 V (see, e.g., Fig. 4 showing the extraction characteristics of the parent and several fragment ions in CF_2Cl_2). Extrapolation of the measured extraction characteristics gives the approximate saturation value needed (see also similar findings and procedures by Schutten et al. [11], where highly energetic protons from H_2O could not be detected in saturation and a correction of ca. 5% had been estimated). It is found that the values measured at around $U_{C-L_2} = 300$ V for the S^+, F^+ and CCl^+ ions have to be corrected by 20%, for the Cl^+, CF^+, FCl^+ ions by 15%, and for the Cl_2^+, CF_2^+, $CFCl^+$ and CCl_2^+ ions by 10% , respectively.

* It is interesting to note that these second peaks do not change the results of the integration process dramatically; both methods tested gave similar results within the quoted error bars.

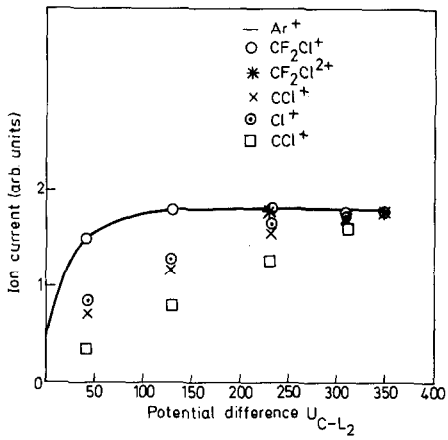

Fig. 4. Integrated (y and z direction) ion currents (using automatic y integration) as a function of the potential difference between the collision chamber C and the lens L_2. Also shown in one case (CCl^+, designated □) the ion current extraction characteristic without any integration. Note the absence of any saturation (for an explanation of this effect see ref. 8). Curves are normalized to the ion current at 340 V.

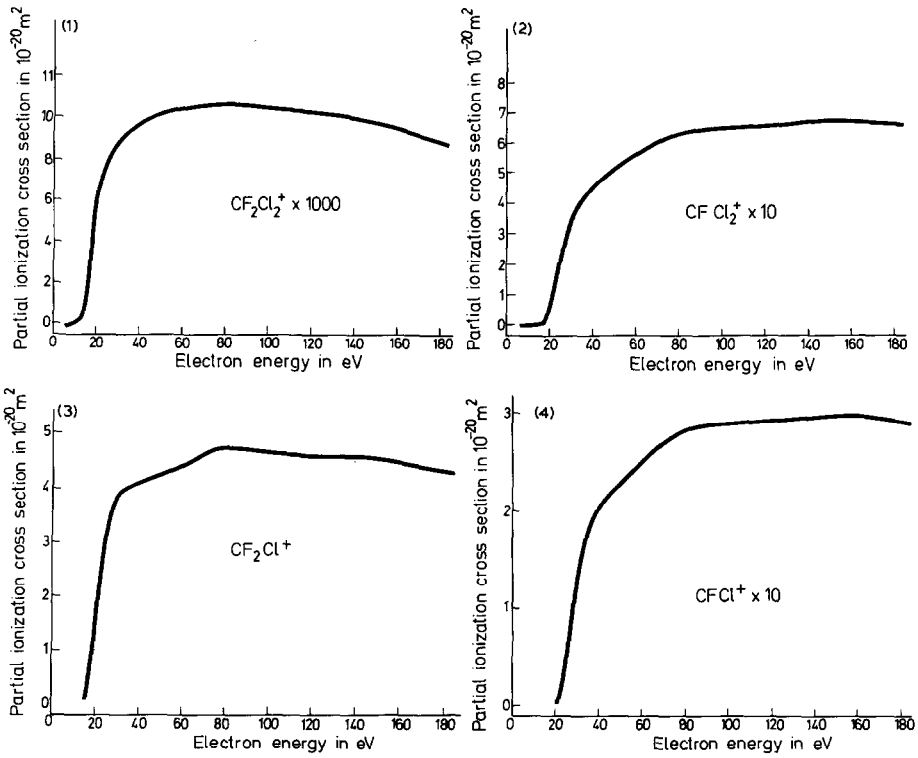

Fig. 5. Absolute partial ionization cross-sections in CF_2Cl_2 as a function of electron energy.

All measurements have been made under saturation-extraction conditions and using the above described integration over y and z directions. The automatic integration method has been tested successfully with the well-known cross-sections in Ar [8,12], i.e., using the relative cross-section function of Ar^+ and the cross-section ratio between Ar^+ and Ar^{2+}. Ion currents, electron current, and the gas pressure in the ion source and in the gas reservoir (which were kept constant) were recorded simultaneously in a data acquisition unit. Typically in one run a total of 400 values of each of these parameters was recorded at about 100 different values of the electron energy.

Calibration processes

The energy scales of the singly charged CF_2Cl_2 ions are absolutely calibrated using linear extrapolation of the Ar^+ cross-section to the ionization energy of Ar^+, whereas the energy scales of the doubly charged ions of CF_2Cl_2 are calibrated against the Ar^{2+} cross-section onset using the square

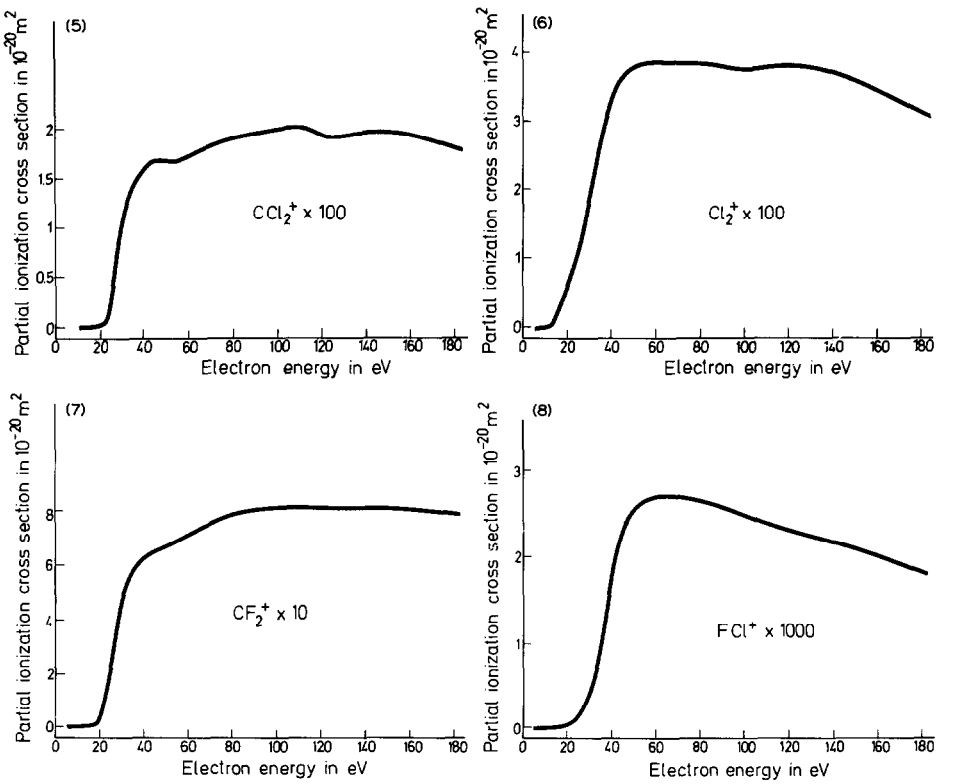

Fig. 5 (continued).

root extrapolation method. This allows us to achieve an electron energy accuracy of ± 0.2 eV.

The absolute calibration of the measured relative partial ionization cross-section functions is a difficult experimental task [1,13], because it necessitates the accurate measurement of the ion current, the number gas density, the collision path length, and the current (density) of the bombarding electrons. Instead of measuring all these quantities, we have used a normalization procedure in which the cross-section to be determined, e.g., $q(CF_2Cl^+/CF_2Cl_2)$, is normalized against the Ar^+ cross-section [8] at one particular electron energy, i.e., the electron impact ionization is measured for both gases (ions) under identical conditions (collision path length and electron current) and for known gas densities, and hence the measured ion current ratio corrected for the respective gas densities can be set equal to the corresponding cross-section ratio [14,15].

This normalization requires the measurement of the gas density of Ar and CF_2Cl_2 in the collision chamber, which is made with the help of the method

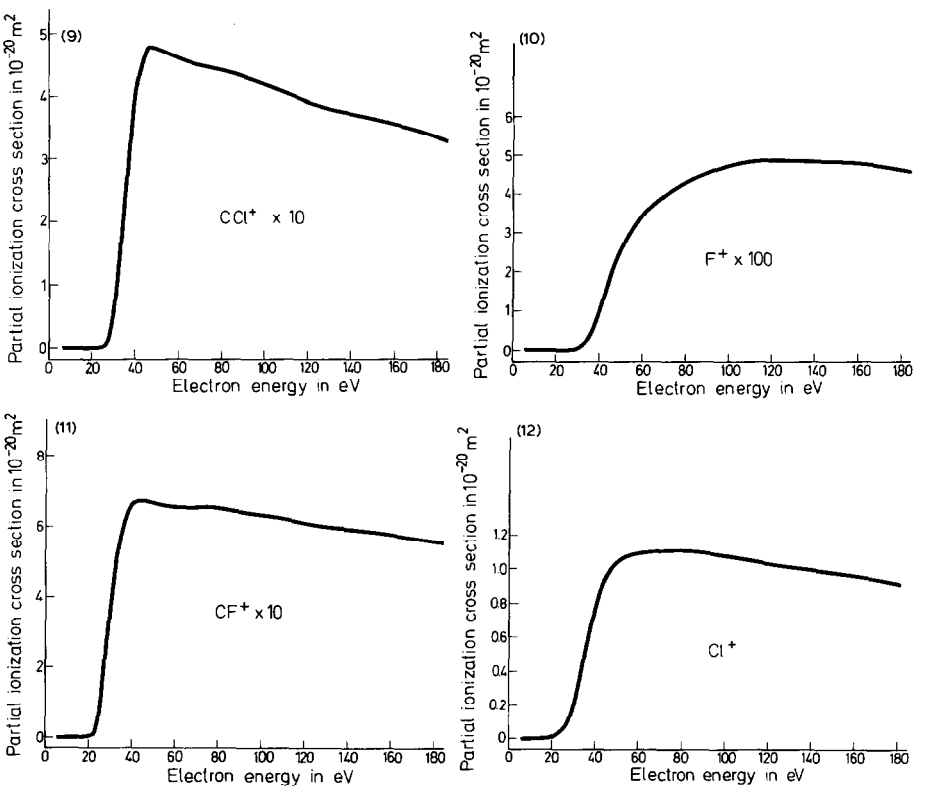

Fig. 5 (continued).

of molecular effusive flow [14,15]. This method relies on the validity of free (collisionless) molecular effusive flow (Knudsen number $K = \lambda_0/D > 10$, with λ_0 mean free path of the gas and D diameter of orifice) from the gas reservoir through the nozzle into the collision chamber and from there to the high vacuum pumps. Under these conditions the gas density ratio in the collision chamber Ar/CF_2Cl_2 is equal to the pressure ratio in the gas reservoir $p(Ar)/p(CF_2Cl_2)$. At equal gas densities we obtain at 100 eV an ion current ratio of 1.4 ± 0.2 between CF_2Cl^+ ($m/z = 85$) and Ar^+ ($m/z = 40$). Taking into account the respective isotope ratios and using $q(Ar^+/Ar) = 2.46 \times 10^{-20}$ m^2 [8] we obtain $q(CF_2Cl^+/CF_2Cl_2) = 4.6 \times 10^{-20}$ m^2 at 100 eV. The other ions of CF_2Cl_2 were calibrated against CF_2Cl^+, hence avoiding any further gas pressure measurements.

RESULTS AND DISCUSSION

Partial ionization cross-section functions (fragmentation patterns)

The absolute partial ionization cross-sections obtained in the present study (for a preliminary presentation of these data see ref. 16) are shown in

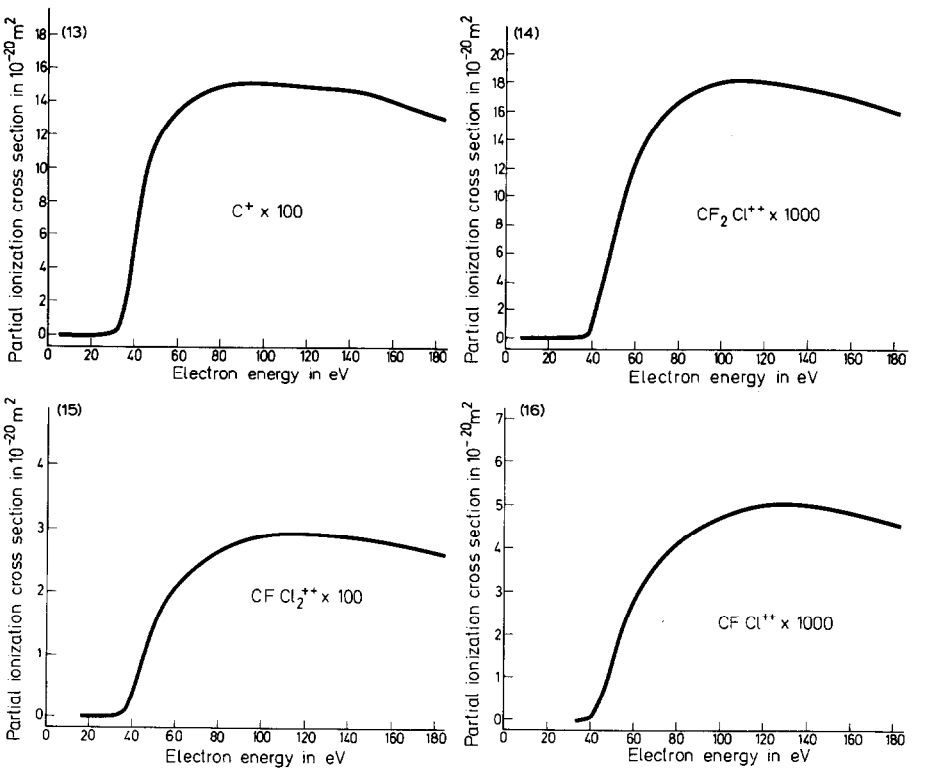

Fig. 5 (continued).

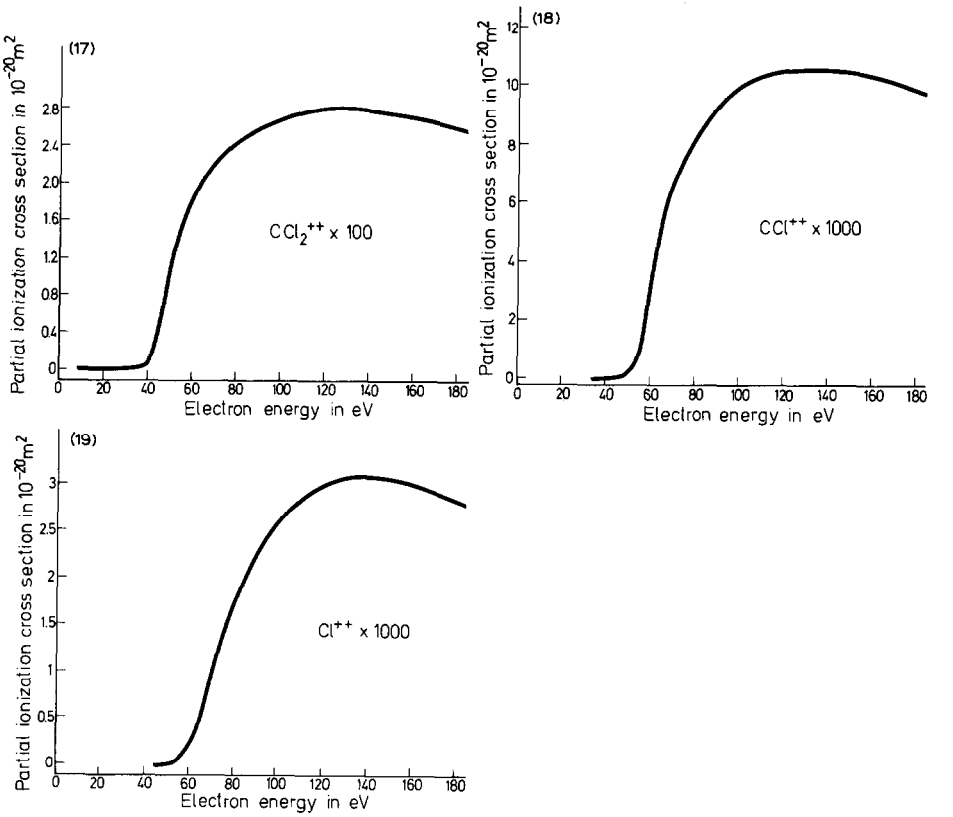

Fig. 5 (continued).

Fig. 5 as a function of electron energy. A representative set of values of these cross-sections is given in Table 1. The maximum relative error is estimated to be $\pm 5\%$ for singly charged ions, and $\pm 10\%$ for doubly charged ions. The error of the absolute values, including the errors involved in the calibration process, is estimated to be approximately 10% for singly charged ions and approximately 20% for doubly charged ions. To the authors' knowledge there exists no previous determination of these cross-section functions. It is interesting to note that, in contrast to CF_4 and CCl_4, parent ions may be detected in CF_2Cl_2 with the mass spectrometer, albeit, with a rather small cross-section.

Total ionization cross-section function

The charge weighted sum of the absolute partial ionization cross-sections (summation method [1]) gives the absolute total ionization cross-sections

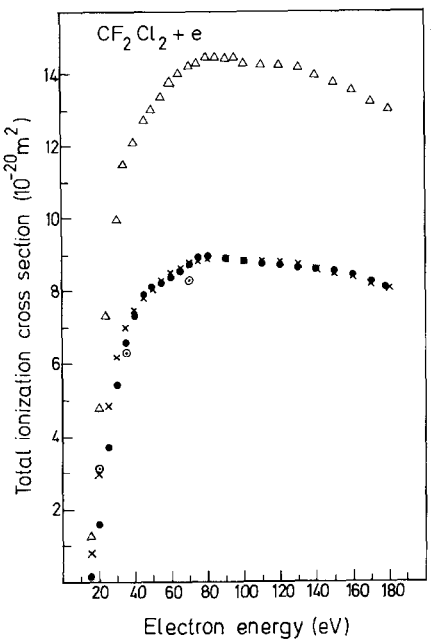

Fig. 6. Absolute total ionization cross-sections in CF_2Cl_2 as a function of electron energy: ●, present results; ⊙, Beran and Kevan [17] renormalized to data of Rapp and Englander-Golden [18]; ×, Pejcev et al. [19] renormalized to the present results at 100 eV; △ Pejcev et al. [19] (see text).

(see Fig. 6 and q_t, Table 1). The relative error of this cross-section function is estimated to be ca. ±5%, whereas for the absolute values an error of approximately ±10% has to be assumed. Also shown in Fig. 6 are values reported by Beran and Kevan [17] for the total ionization cross-section measured at 20, 35 and 70 eV. These values have been renormalized to the established total ionization cross-sections in argon reported by Rapp and Englander-Golden [18]. Similar to other cases [6], these renormalized values are in good agreement with our values. Figure 6 shows furthermore the ionization cross-section curve reported by Pejcev et al. [19]. These values have been measured with a parallel plate condenser type ionization chamber. As in the case of another gas [20] their values are almost a factor of two larger than our data. On the other hand, if their data are normalized to our data (e.g., at 100 eV) very good agreement is obtained between the shapes of these cross-section curves. The difference in magnitude must be due to different calibration procedures. In addition, there exist several calculations on the ionization cross-sections of CF_2Cl_2. The results have been recently summarized by Deutsch et al. [21]. Improved classical and semiclassical binary encounter approximations show good agreement with the present results (see fig. 4 in ref. 21).

TABLE 1

Absolute partial and total ionziation cross-sections as a function of electron energy in m^2

Energy (eV)	$CF_2Cl_2^+$ 10^{-22}	$CFCl_2^+$ 10^{-21}	CF_2Cl^+ 10^{-20}	CCl_2^+ 10^{-22}	Cl_2^+ 10^{-22}	$CFCl^+$ 10^{-21}	FCl^+ 10^{-23}	CF_2^+ 10^{-21}	CCl^+ 10^{-21}	Cl^+ 10^{-20}
15	0.09		0.12		0.16					
20	0.63	0.70	1.44	0.01	0.61		0.04	0.28		
25	0.76	2.25	3.02	0.33	1.01	0.59	0.13	2.43		0.05
30	0.89	3.52	3.78	1.00	1.75	1.37	0.46	4.62	0.59	0.21
35	0.93	4.11	3.99	1.40	2.68	1.87	0.89	5.83	2.35	0.51
40	0.97	4.47	4.05	1.60	3.29	2.12	1.79	6.32	4.03	0.78
45	1.00	4.82	4.17	1.67	3.60	2.23	2.36	6.56	4.75	0.97
50	1.02	5.10	4.21	1.67	3.78	2.31	2.55	6.64	4.81	1.06
55	1.04	5.31	4.28	1.67	3.83	2.42	2.63	6.93	4.70	1.09
60	1.05	5.56	4.39	1.70	3.83	2.54	2.69	7.13	4.63	1.10
65	1.05	5.73	4.48	1.78	3.81	2.63	2.69	7.33	4.55	1.09
70	1.06	5.98	4.60	1.83	3.80	2.72	2.68	7.57	4.53	1.10
75	1.06	6.12	4.72	1.88	3.81	2.81	2.67	7.78	4.49	1.11
80	1.07	6.26	4.72	1.90	3.83	2.88	2.65	7.80	4.44	1.12
90	1.06	6.37	4.66	1.96	3.76	2.90	2.56	8.02	4.36	1.09
100	1.10	6.40	4.60	2.06	3.70	2.90	2.50	8.10	4.20	1.08
110	1.04	6.44	4.58	2.02	3.76	2.93	2.40	8.10	4.08	1.06
120	1.03	6.51	4.54	1.91	3.80	2.94	2.31	8.06	3.94	1.04
130	1.02	6.54	4.54	1.93	3.75	2.97	2.24	8.10	3.80	1.02
140	1.00	6.61	4.54	1.96	3.70	2.98	2.18	8.10	3.75	1.01
150	0.98	6.68	4.52	1.96	3.56	2.98	2.12	8.10	3.66	0.98
160	0.95	6.68	4.44	1.93	3.43	2.99	2.04	8.06	3.58	0.97
170	0.93	6.61	4.35	1.87	3.29	2.97	1.92	8.02	3.49	0.94
180	0.89	6.58	4.28	1.82	3.11	2.95	1.83	7.94	3.37	0.92

TABLE 1 (continued).

Energy (eV)	CF^+ 10^{-21}	F^+ 10^{-22}	C^+ 10^{-21}	Cl^{2+} 10^{-23}	CCl^{2+} 10^{-22}	CCl_2^{2+} 10^{-22}	$CFCl^{2+}$ 10^{-23}	CF_2Cl^{2+} 10^{-22}	$CFCl_2^{2+}$ 10^{-22}	q_t 10^{-20}
15										0.12
20										1.55
25	0.55									3.67
30	3.60	0.03	0.02							5.40
35	5.79	0.27	0.13							6.56
40	6.71	0.87	0.53			0.06	0.04	0.09	0.34	7.32
45	6.86	1.89	1.10			0.45	0.52	0.39	0.99	7.88
50	6.71	2.57	1.16			1.07	1.04	0.71	1.50	8.07
55	6.55	3.01	1.26	0.06	0.15	1.52	2.21	1.00	1.88	8.22
60	6.58	3.36	1.32	0.19	0.31	1.88	2.74	1.23	2.10	8.43
65	6.58	3.66	1.39	0.48	0.54	2.08	3.21	1.39	2.29	8.57
70	6.61	3.88	1.42	0.91	0.66	2.25	3.58	1.51	2.44	8.76
75	6.64	4.10	1.46	1.34	0.74	2.37	3.88	1.60	2.58	8.95
80	6.61	4.24	1.46	1.64	0.81	2.46	4.08	1.67	2.66	8.99
90	6.49	4.51	1.51	2.15	0.91	2.61	4.43	1.76	2.82	8.92
100	6.40	4.70	1.50	2.50	0.99	2.70	4.70	1.80	2.90	8.84
110	6.31	4.81	1.49	2.72	1.02	2.78	4.87	1.82	2.93	8.78
120	6.10	4.84	1.48	2.87	1.03	2.81	4.97	1.80	2.92	8.76
130	6.03	4.81	1.47	2.94	1.03	2.83	4.99	1.78	2.90	8.66
140	6.00	4.81	1.47	2.96	1.04	2.79	4.97	1.76	2.88	8.65
150	5.94	4.81	1.44	2.93	1.03	2.77	4.92	1.72	2.85	8.59
160	5.85	4.75	1.39	2.87	1.02	2.74	4.85	1.69	2.78	8.46
170	5.73	4.67	1.34	2.79	0.99	2.68	4.73	1.65	2.71	8.31
180	5.64	4.59	1.31	2.72	0.98	2.62	4.60	1.60	2.64	8.17

ACKNOWLEDGEMENTS

This work was partially supported by Österreichischer Fonds zur Förderung der Wissenschaftlichen Forschung. It is a pleasure to thank Dr. Kurt Stephan, Universitätsklinik für Hörstörungen, Universität Innsbruck, for helpful discussion and assistance.

REFERENCES

1 T.D. Märk and G.H. Dunn, Electron Impact Ionization, Springer, Wien, 1985.
2 R.S. Freund, in L.C. Pitchford, B.V. McKoy, A. Chutjian and S. Trajmar (Eds), Swarm Studies and Inelastic Electron–Molecule Collisions, Springer, New York, 1987, pp. 329–346.
3 H.U. Poll and J. Meichsner, Contrib. Plasma Phys., 27 (1987) 359.
4 D.L. Flamm and V.L. Donnelly, Plasma Chem. Plasma Proc., 1 (1981) 317 (and references cited therein).
5 U. Prösch and K. Buttke, Beitr. Plasmaphys., 24 (1984) 645.
6 K. Stephan, H. Deutsch and T.D. Märk, J. Chem. Phys., 83 (1985) 5712.
7 K. Leiter, K. Stephan, E. Märk and T.D. Märk, Plasma Chem. Plasma Proc., 4 (1984) 235.
8 K. Stephan, H. Helm and T.D. Märk, J. Chem. Phys., 73 (1980) 3763.
9 T.D. Märk, Beitr. Plasmaphys., 22 (1982) 257.
10 T.D. Märk, Int. J. Mass Spectrom. Ion Phys., 45 (1982) 125.
11 J. Schutten, F.J. de Heer, H.R. Moustafa, A.J.H. Boerboom and J. Kistemaker, J. Chem. Phys., 44 (1966) 3924.
12 T.R. Hayes, R.C. Wetzel, F.A. Baiocchi and R.S. Freund, Phys. Rev. A, 32 (1987) 559.
13 L.J. Kieffer and G.H. Dunn, Rev. Mod. Phys., 38 (1966) 1.
14 C.E. Brunnee and V. Voshage, Massenspektrometrie, Thiemig, Munich, 1964.
15 T.D. Märk, J. Chem. Phys., 63 (1975) 3731.
16 K. Leiter and T.D. Märk, Presentation at 7th Int. Symp. Plasma Chemistry, Eindhoven, The Netherlands, 1985.
17 J.A. Beran and L. Kevan, J. Phys. Chem., 73 (1969) 3866.
18 D. Rapp and P. Englander-Golden, J. Chem. Phys., 43 (1965) 1464.
19 V.M. Pejcev, M.V. Kurepa and I.M. Cadez, Chem. Phys. Lett., 63 (1979) 301.
20 N. Djuric, D. Belic, M. Kurepa, J.U. Mack, J. Rothleitner and T.D. Märk, 12th ICPEAC, Gatlinburg, TN, 1981, p. 384.
21 H. Deutsch, P. Scheier and T.D. Märk, Int. J. Mass Spectrom. Ion Processes, 74 (1986) 81.